



Continuous vs. pulsating flow boiling. Part 1: Experimental comparison and visualization

Kærn, Martin Ryhl; Elmegaard, Brian; Meyer, Knud Erik; Palm, Björn

Published in:

Proceedings of the 16th International Refrigeration and Air Conditioning Conference

Publication date:

2016

Document Version

Peer reviewed version

[Link back to DTU Orbit](#)

Citation (APA):

Kærn, M. R., Elmegaard, B., Meyer, K. E., & Palm, B. (2016). Continuous vs. pulsating flow boiling. Part 1: Experimental comparison and visualization. In *Proceedings of the 16th International Refrigeration and Air Conditioning Conference* (pp. 1310-1318). [2513] Ray W. Herrick Laboratories.
<https://docs.lib.purdue.edu/iracc/1781/>

General rights

Copyright and moral rights for the publications made accessible in the public portal are retained by the authors and/or other copyright owners and it is a condition of accessing publications that users recognise and abide by the legal requirements associated with these rights.

- Users may download and print one copy of any publication from the public portal for the purpose of private study or research.
- You may not further distribute the material or use it for any profit-making activity or commercial gain
- You may freely distribute the URL identifying the publication in the public portal

If you believe that this document breaches copyright please contact us providing details, and we will remove access to the work immediately and investigate your claim.

Continuous vs. pulsating flow boiling. Part 1: Experimental comparison and visualization

Martin Ryhl Kærn^{1*}, Brian Elmegaard¹, Knud Erik Meyer¹, Björn Palm²

¹Technical University of Denmark, Department of Mechanical Engineering, Kongens Lyngby, Denmark,
Tel: +45 4525 4121, Fax: +45 4593 5215, Email: pmak@mek.dtu.dk

²Royal Institute of Technology, Department of Energy Technology, Stockholm, Sweden

ABSTRACT

This experimental study investigates an active method for flow boiling heat transfer enhancement by means of fluid flow pulsation. The hypothesis is that pulsations increase the flow boiling heat transfer by means of better bulk fluid mixing, increased wall wetting and flow-regime destabilization. The fluid pulsations are introduced by a flow modulating expansion device and are compared with continuous flow by a stepper-motor expansion valve in terms of time-averaged heat transfer coefficient. The cycle time ranges from 1 s to 9 s for the pulsations. The time-averaged heat transfer coefficients are reduced from transient measurements immediately downstream of the expansion valves at low vapor qualities. The results show that the pulsations improve the time-averaged heat transfer coefficient by 3.2 % on average at low cycle time (1 s to 2) s, whereas the pulsations may reduce the time-averaged heat transfer coefficient by as much as 8 % at high heat flux ($q \geq 35 \text{ kW/m}^2$) and cycle time (8 s). The latter reduction is adhered to the significant dry-out when the flow modulating expansion valve is closed.

1. INTRODUCTION

High heat exchanger performance is crucial to meet efficiency standards with low cost and environmental impact in various applications such as heat pumps, refrigeration and air-conditioning. The performance of heat exchangers may be improved by passive and active heat transfer enhancement techniques applicable to air, liquid and phase change heat exchangers. In the current paper, an experimental investigation of flow boiling heat transfer is conducted in a traditional round-tube evaporator with the aim of heat transfer enhancement by means of fluid flow pulsations. The pulsations are generated by a flow-modulating expansion valve. The refrigerant is chosen to be R134a, i.e. a well-examined pure fluid with respect to steady continuous flow boiling heat transfer measurements.

The field of heat transfer enhancement is enormous in the literature and many reviews have been given in even small narrow subjects. Some examples of more broad reviews on various heat transfer enhancement techniques are the reviews given by Bergles (2003) and Ohadi *et al.* (1996). They indicated that fluid pulsation (or fluid vibration as denoted by these authors) had received little attention at that time in the literature for boiling and condensation enhancement, and that the results had not been promising so far. Antonenko *et al.* (1992) found that the developed nucleate boiling region was impossible to enhance by fluid vibrations at 15 Hz to 100 Hz. They argued that the superheated layer near the wall was destroyed which led to the suppression of the bubble formation. However, in other modes of heat transfer, like convective heat transfer and film boiling, enhancement was as much as 50 %. Obinelo *et al.* (1994) studied steam pulsations (0.08 Hz to 0.25 Hz) in a reflux condenser and found that the induced pulsations had a destabilizing effect on the water column and led to a several-fold increase in the condensation capacity.

Bohdal and Kuczyński (2005) investigated flow oscillations in an R134a evaporator coil. The periodically generated disturbances were created by a flow-modulating valve with a constant opening time at 5 s and closing times from 5 s to 30 s (cycle times: 10 s to 35 s). They found that the superheated region increases with the cycle time and leads to a decrease in the heat transfer performance. Later, the same authors (Kuczyński *et al.*, 2012) investigated flow oscillation during condensation of R134a in pipe mini-channels with 0.64 mm to 3.3 mm diameter. The cycle times

were lower compared to the earlier study. It ranged from 0.2 s to 4 s with equal opening and closing times. They found that the subcooling area in the condenser increased with increasing cycle time, while the condensation area decreased and led to a reduction of the overall condenser effectiveness.

Chen *et al.* (2010) studied time-periodic flow boiling of R134a in a narrow annular duct with 2 mm gap. The imposed mass flow oscillations were nearly triangular waves with peak-to-peak amplitudes from 10 % to 30 % of the average flow and cycle times from 30 s to 120 s. Only a slight impact on the time-averaged heat transfer coefficient and boiling curve was observed at these modest oscillations. Roh and Kim (2012) conducted an experimental study on the system performance enhancement of a R410A heat pump using an additional solenoid-driven expansion valve in parallel with the main expansion valve. The additional expansion valve was periodically opened for only 200 ms at cycle times ranging from 5 s to 200 s. The coefficient of performance (COP) was improved by up to 4 %. The authors claimed the enhancement was caused by both the pulsation enhanced heat transfer and the so-called “pushing effect” that elevated the compressor suction and discharge pressures immediately after each pulse, thereby reducing the compression ratio.

Various forms of dynamic two-phase flow instability have been recognized in the literature (Ruspini *et al.* 2014), and they should be mentioned in relation to the current investigation, although these occur in the nuclear industry where only the liquid and two-phase regions exist. The two major modes of these dynamic oscillations are density-wave type (high frequency) and pressure-drop type (low frequency) oscillation. The former is caused by the dynamic interaction between pressure drop, flow rate and local density variation, and is characterized by large variations in outlet vapor quality and mass flow rate. The latter is caused by the S-shape pressure drop vs. mass flow rate characteristics of two-phase flow systems and occurs specifically when a compressible volume is located upstream or distributed within the boiling channel, so as to cause mass flow oscillation. These oscillations are not expected to occur in dry-expansion systems with superheated vapor generation. In these systems, a well-known phenomenon called hunting is sometimes encountered if a thermostatic expansion valve is used. Even in steady operation, the transition point from two-phase to vapor phase oscillates (Wedekind, 1971), resulting in oscillation of superheat and thus valve opening degree. Even for electronic expansion valves, a minimum degree of superheat must be ensured for a stable superheat signal and system operation.

The objective of the current paper is to demonstrate the possible heat transfer enhancement with flow pulsations, by comparing the pulsatile flow boiling heat transfer results with that of continuous flow boiling for low qualities, i.e. immediately downstream of the pulsation source with apparently the strongest pulsation strength. The oscillating dryout location and associated effects on the heat transfer performance is not considered herein. The hypothesis is that the pulsations will increase the flow boiling heat transfer by means of better bulk fluid mixing, increased wall wetting and flow-regime destabilization. Two widely accepted flow-boiling mechanisms occur in traditional tubing, namely the nucleate and the convective boiling. The concept of fluid flow pulsation is evidently linked to both these mechanisms. The convective boiling term is believed to enhance due to fluid pulsation, while the nucleate boiling is believed to decrease due to increased suppression or loss of wall superheat.

2. EXPERIMENTAL APPARATUS

The experimental apparatus is illustrated in Figure 1. The pump bypass loop circulates at least 5 times the refrigerant needed for the test-section. The stepper motor bypass valve controls the high pressure liquid to the test section whereas the low pressure is controlled by an oversized condenser, and accordingly the temperature of the refrigerated glycol. The high pressure liquid ($T_{\text{sat}} = 32^{\circ}\text{C}$) is led through a Siemens SITRANS FC300 Coriolis-type mass flow meter with an accuracy of 0.14 % and heated to 30°C by an oversized liquid heater. To avoid spurious oscillating mass flow readings, two pulsation dampers are installed both upstream and downstream of the mass flow meter. The subcooled liquid is expanded down to low-pressure two-phase flow ($T_{\text{sat}} = 5^{\circ}\text{C}$) by exchangeable expansions valves, namely the flow modulating expansion valve (Danfoss AKV) and the stepper-motor expansion valve (Danfoss ETS). Two 200 mm long glass-tube-sections with external vacuum chambers are installed upstream and downstream the test section to visualize the flow with high-speed camera. The upstream glass section is located about 120 mm downstream the throat areas in the expansion valves. The remaining liquid is evaporated in an auxiliary evaporator and led back to the pump bypass.

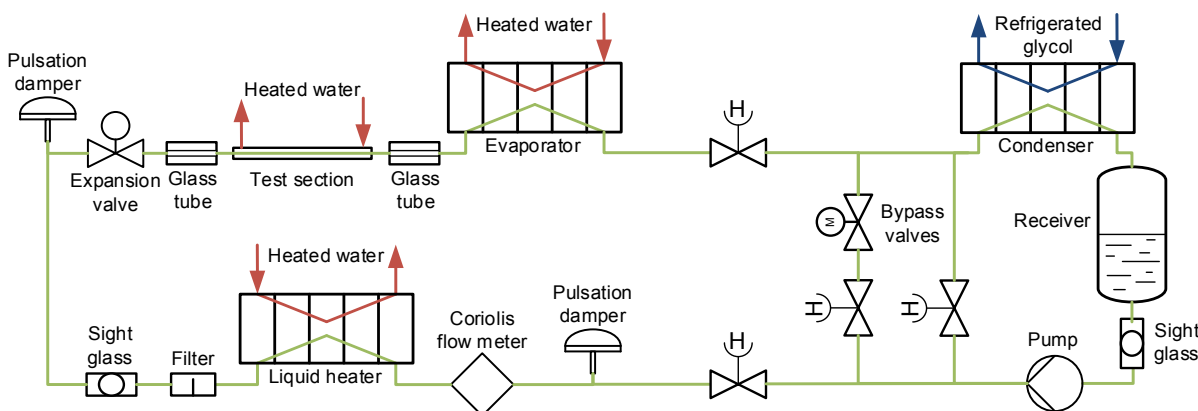


Figure 1: Experimental apparatus (H: hand-operated valve)

The test-section is sketched in Figure 2 including temperature and pressure sensors. It is a co-axial type evaporator with refrigerant R134a flowing in the inner tube and distilled water flowing outside helically through four sub-sections, and allows computing four heat transfer coefficients for each steady state reading. We use hot water instead of electrical heat to heat-up the evaporator for the following reason: The liquid dry-out of the inner wall surface would increase the wall temperature rapidly, if electrical heaters were used, and possibly reach impractical temperatures in typical evaporators, when the flow modulation valve is closed. On the contrary, the wall temperature will always be limited by the hot water temperature, when hot water is used.

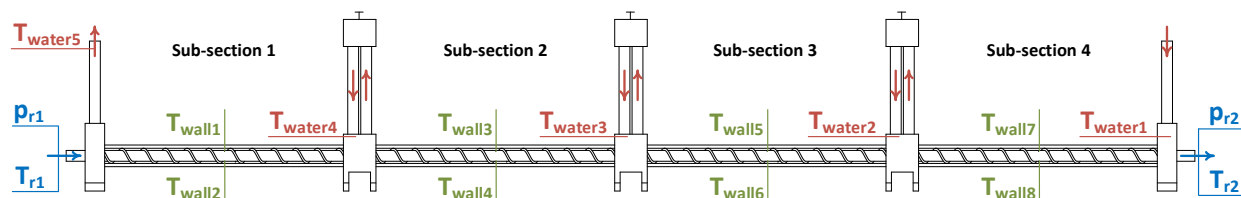


Figure 2: Test section including each sub-section

The inner tube internal and external diameters were 8 mm and 10 mm, respectively, and the outer tube inner diameter was 14 mm. The water was led away from the annulus and through PTFE static mixers in order to measure a well-mixed average temperature before entering the next sub-section. The helical flow was arranged by folding a 2 mm capillary copper tube in a spiral shape before inserting it into the outer transparent acrylic tube during assembly and this allowed for an even helical angle specified to 30 degrees. The transparent outer tube allowed for a visual inspection of air bubbles before the measurements were recorded. Wall temperatures were measured externally at the top and bottom of the inner tube in the center of each sub-section by soldering 0.5 mm sheathed thermocouples (Omega Engineering type-T with special limits of error) into 10 mm grooves along the tube. Special attention was given to avoid any additional thermal capacitance in contact with the inner tube wall in the current design in order to capture wall temperature oscillation due to flow pulsation. Only small parts in the test section (e.g. o-rings) were allowed to be in contact with the inner tube and all connecting blocks were made of PVC. The capillary tube had a small mass and small contact area with the inner tube too. Saturation pressures and temperatures were measured upstream and downstream the test-section. The cold junctions of the thermocouples were installed into an ice-point reference and the hot junction readings were calibrated against a standard resistance thermometer using a calibration bath to an accuracy of 0.031 K before installation. The temperature readings were performed by National Instruments CompactDAQ module 9214 configured in high-speed mode in order to resolve the temperature transients due to flow pulsation. It resulted in a poorer accuracy (0.1 K) due to the increased sensitivity of measuring in high-speed mode. All thermocouples were recorded at 10 Hz. The pressure transmitters were also calibrated using a dead-weight tester and found to have a hysteresis within 150 Pa and an accuracy of 0.081 % FS (6 bar) and 0.091 % FS (10 bar) for the low and high-pressure transmitters, respectively. National Instruments CompactDAQ module 9203 was used to read both refrigerant mass flow and pressure at 1000 Hz. The water flow rates were measured by an oval-gear volume flow meter with an accuracy of 0.26 % FS (1 L/min) and read by National Instruments CompactDAQ module 9411.

2.1 Data reduction

The data reduction is similar to the method used by Wojtan *et al.* (2005). It is based on a regression of the time-averaged water flow enthalpies allowing for the time-averaged local heat flux evaluation by differentiation.

$$q(z) = \frac{\rho_w \dot{V}_w}{\pi d} \frac{dh_w}{dz} - q_\infty \quad (1)$$

Where ρ_w , h_w and \dot{V}_w are the density, enthalpy and volume flow rate of water, d is the inner tube internal diameter and q_∞ is the sub-section averaged heat loss/gain through the outer insulation. This value was always calculated to be below 2 W. We found the best regression using the power based form: $h_w = a(z+b)^c$, where a , b and c are coefficients of the regression. The heat transfer coefficient is then computed by

$$\frac{1}{\alpha(z)} = \frac{T_{\text{wall}} - T_{\text{sat}}}{q(z)} - \frac{\ln(D/d)/d}{2k} \quad (1)$$

Where T_{sat} is the saturation temperature evaluated by the measured time-averaged saturation pressure, T_{wall} is the time-averaged wall temperature, D is the outer diameter and k is the thermal conductivity of the copper tube.

Figure 3a shows the calculated values and errors using the error propagation method by Kline and McClintock (1953) for the continuous flow experiments. Note that the heat transfer coefficients from sub-section 1 are omitted, because one of the wall temperature sensors was broken during installation. The absolute errors ranged from (54 to 143) W/m²K and (141 to 390) W/m² for the heat transfer coefficient and heat flux, respectively. Percentagewise the errors became as much as 10 % when approaching zero heat flux. Above 2 kW/m²K, the heat transfer coefficient predictions had errors below 3.8 %. The absolute error in the local vapor quality calculations was always below 0.006. Liquid-liquid tests were also conducted in the test-section to ensure the reliability of the data reduction method. These tests showed a mean absolute deviation (MAD, see Eqn. 5 in part 2 of this paper) of 6.5 % with the correlation by Gnielinski at Reynolds numbers from 3800 to 6100. These tests also revealed that the solenoid-driven flow-modulating valve released a nearly constant heat input of 6 W at 100 % opening degree for all refrigerant flow rates. Ideally, the stepper-motor should not draw any current in a given steady state.

Figure 3a indicates that the current heat transfer coefficients are weak functions of mass flux and strong functions of heat flux. This indicates that nucleate boiling dominates over convective boiling. Furthermore, the power relation of the lowest mass flux tests ($G \leq 50$ kg/m²) shows that $\alpha \propto q^{0.66}$, which corresponds well with the equation proposed in the VDI Heat Atlas for nucleate boiling: $n(p^*) = 0.8 - 0.1 \cdot 10^{(0.76 p^*)} = 0.68$. Since the convective boiling contribution is low, there may be incentive to augment this contribution by flow pulsation. On the other hand, the nucleate boiling may decrease as well due to increased suppression by convection. Note that the refrigerant state at the inlet to the test section is similar in all the experiments. As a result, the vapor quality and heat flux are correlated (or non-orthogonal). This is discussed in more detail in part 2 of this paper.

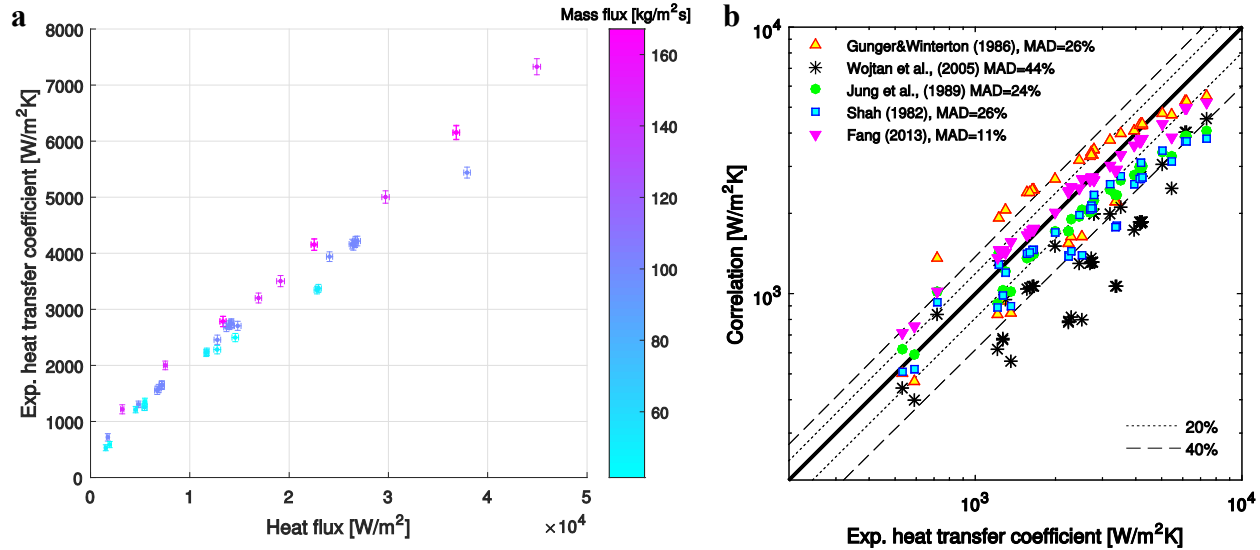


Figure 3: Experimental heat transfer coefficients vs. heat flux (a) and vs. predictions from correlations (b) for the continuous flow experiments

The heat transfer coefficients for the continuous two-phase flow experiments is compared with correlations in the literature in Figure 3b including each MAD. It shows that the current experimental heat transfer coefficients are in good agreement with the correlations, except for the phenomenological correlation by Wojtan *et al.* (2005), which shows a MAD of 44 %. The recently developed correlation by Fang (2013) predicts our results the best (MAD = 11 %), however, it was also specifically developed for R134a in contrast to the others.

3. RESULTS

In this section, the heat transfer coefficients with and without flow pulsation are compared. Visualizations with high-speed camera are also presented that illustrates both pros and cons regarding the pulsations.

3.1 Comparison of heat transfer coefficients

The inlet refrigerant state to the test section is similar in all of the experiments conducted in this work, and resulting from the fixed saturation temperature of 5 °C and the refrigerant state before the expansion valve. Similarly, the inlet water temperature is kept constant at 25 °C. Both the refrigerant mass flux and the water flow rate were varied for each expansion valve from (41 to 167) kg/m²s and (0.10 to 0.76) L/min, respectively. The cycle time of the flow-modulating valve was further varied from 1 s to 9 s. These conditions resulted in a time-averaged local vapor quality range of 0.18 to 0.59 (most points 0.18 to 0.42), time-averaged local heat flux range of (1.5 to 45) kW/m² and time-averaged heat transfer coefficient range of (0.5 to 7.3) kW/m²K. The actual experimental design (the data points recorded) are discussed in part 2 of the paper.

The local heat transfer coefficients are compared directly in sub-sections 2 to 4 as functions of the cycle time. The continuous flow results are presented at zero cycle time, for simplicity. To account for variations in the controlled parameters, the entire set of predicted heat transfer coefficients are normalized by the best correlation in Figure 3b (Fang, 2013). The results are shown in Figure 4.

The heat transfer coefficients change less than expected with the cycle time. On the other hand, there is a tendency towards better heat transfer coefficients as the cycle time goes to 1 s (fastest flow modulation performed). For low cycle times (1 s to 2 s), the heat transfer coefficients are always greater than the continuous flow (cycle time = 0), except for a single point ($G = 50$ kg/m²s, $\dot{V}_w = 0.25$ L/min in sub-section 2). The average enhancement by pulsations is 3.2 % for these cycle times. At higher cycle times the enhancement decreases.

An important reduction in the heat transfer coefficient is observed with flow pulsation at high cycle-times and water flow rates and in the 4th sub-section where the water temperature is highest ($G = 150 \text{ kg/m}^2\text{s}$, $\dot{V}_w = 0.76 \text{ L/min}$ and $G = 100 \text{ kg/m}^2\text{s}$, $\dot{V}_w = 0.57 \text{ L/min}$). The heat flux is very high at these conditions ($q \geq 35 \text{ kW/m}^2$) beyond those typically encountered in refrigeration and air-conditioning. Moreover, the liquid film on the wall dries out significantly when the valve is closed. The reduction is as much as 8 % in the time-averaged heat transfer coefficient. This observation will be detailed in Section 3.2. The average enhancement by pulsations is only 0.5 % for cycle times at 5 s to 6 s, however, disregarding the aforementioned high heat flux results, the enhancement is slightly better (1.2 %). The average enhancement for cycle times at 8 s to 9 s is negative (-0.4 %), however, again disregarding the high heat flux results, the enhancement becomes 0.1 %.

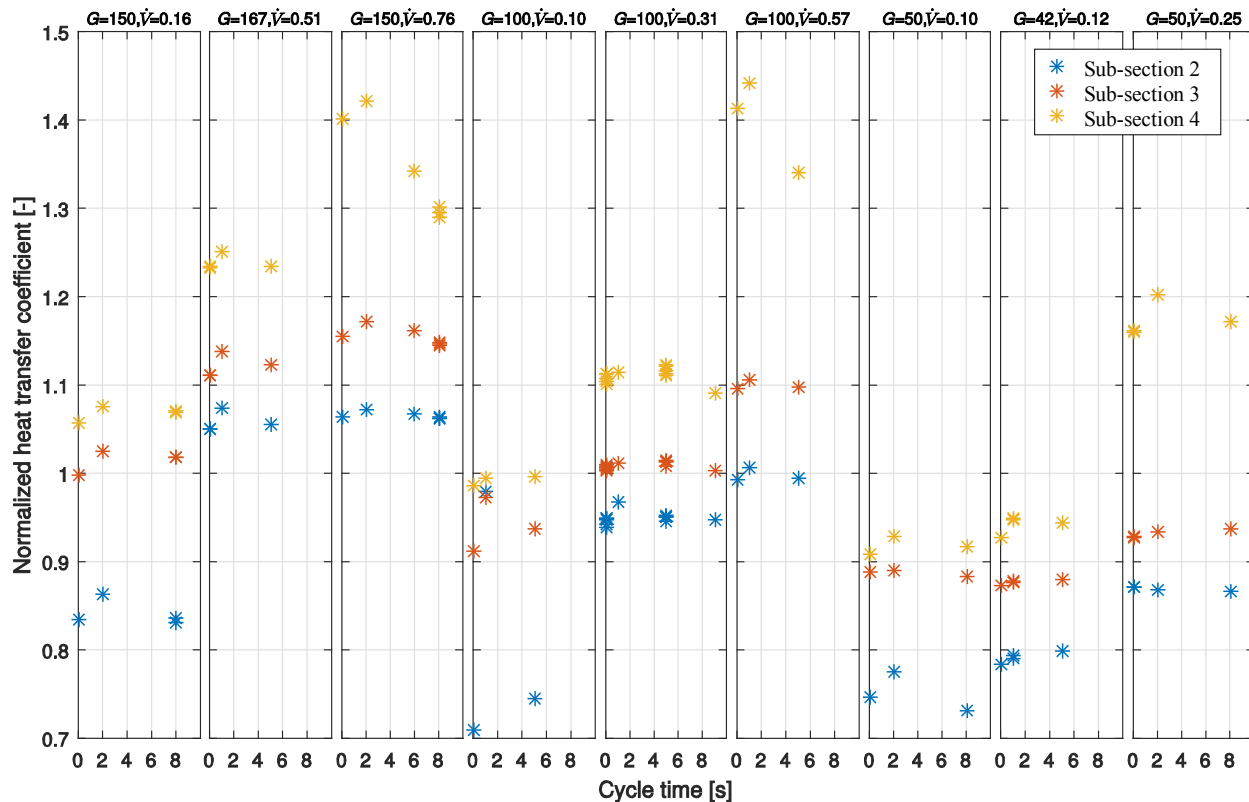


Figure 4: Normalized heat transfer coefficients vs. cycle time at different refrigerant mass fluxes and water volume flows. Continuous flow results located at 0 cycle time.

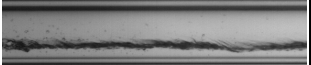
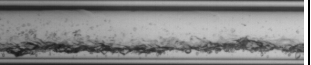
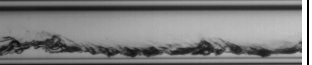
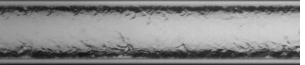

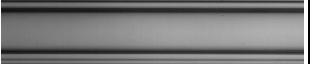
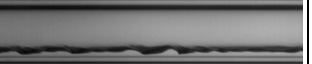
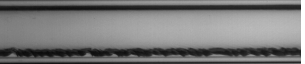
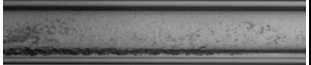
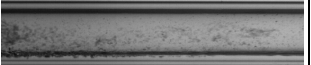
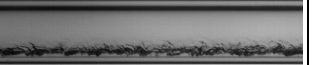
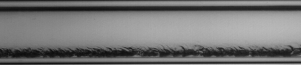
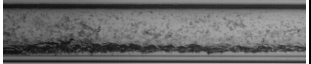
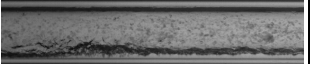
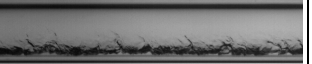

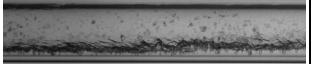
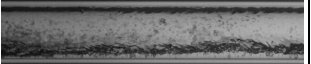
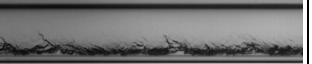
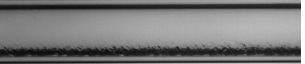
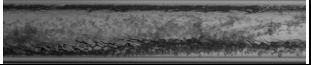
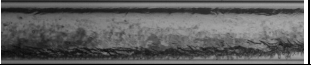
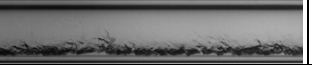
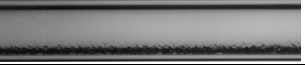
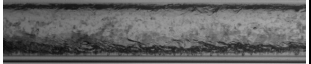
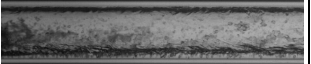
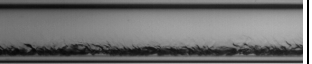
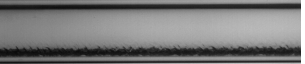
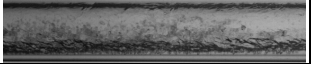
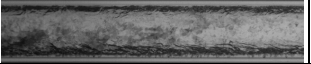
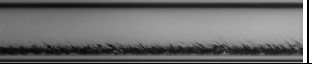
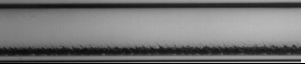
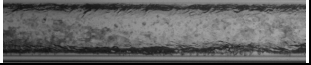
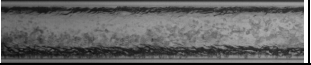
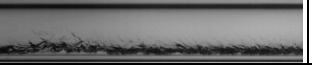
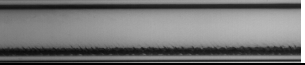
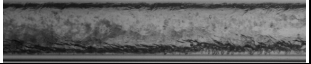
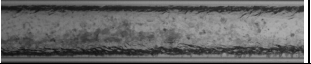
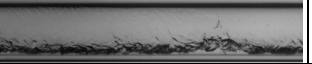
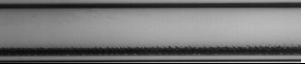


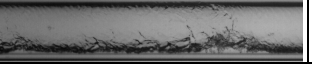
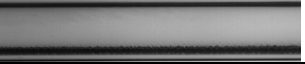


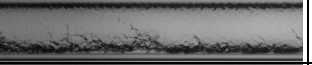
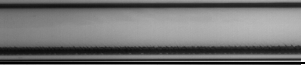


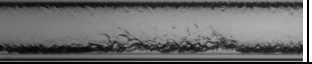
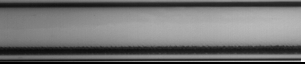


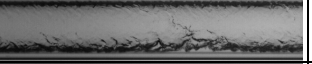
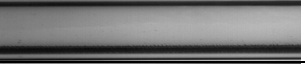


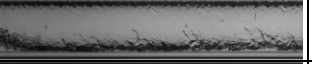
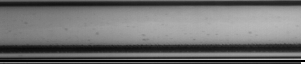


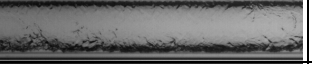
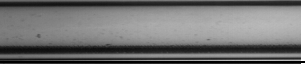


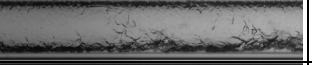
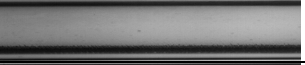
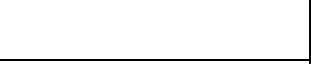
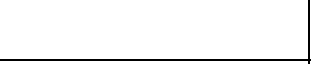
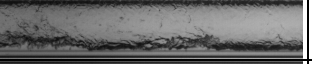
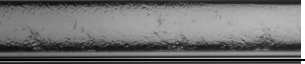


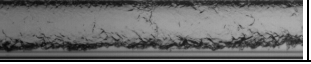
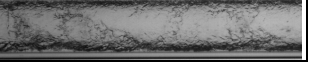
3.2 Visualization

The flow pulsations are visualized upon the opening of the flow modulating expansion valve and shows the liquid injection immediately before and after the test section. To eliminate time delays between the TTL trigger signal for the camera and the valve opening, a DC coil was used for the valve and coupled to an optocoupler for generating the TTL trigger signal for the camera. The pressure change, immediately before and after the expansion valve, occurred with time delays smaller than 10 ms. Table 1 shows the visualizations at two different conditions ($G = 100 \text{ kg/m}^2\text{s}$, $\dot{V}_w = 0.30 \text{ L/min}$ and $G = 150 \text{ kg/m}^2\text{s}$, $\dot{V}_w = 0.76 \text{ L/min}$) with 5 s cycle time each. They are recorded by Photron FastCam-X1280PCI at 1000 fps and 1/16000 s shutter time. The frames are nearly 60 mm wide and resolved by 640 pixels.

The visualizations of the flow pulsations before the test section (case 1 and 2) are very similar. For both cases, a very stagnant liquid film occupies the bottom of the tube before the valve opens. As the valve opens, mist flow occurs in the gas due to flashing through the expansion valve. Waves are formed on the liquid interface due to shear and drags the liquid downstream. Annular flow eventually occurs at around 0.2 s and onwards (developed annular two-phase flow). Stratified-wavy flow with droplets entrained in the gas is shown for the continuous flow with larger wavy character at higher mass flux (case 2).

The visualizations after the test section (case 3 and 4) are much different. For the pulsatile flow, the amount of liquid at the bottom of the tube is significantly different when the valve opens. Moreover, larger amounts of liquid are evaporated when the valve is closed for case 4, because of higher water flow and thus heat flux into the test section. On the other hand, larger waves are present in case 3 with lower heat flux, because of the larger liquid amount, and the flow develops faster too (becomes annular at 0.7 s and onwards). For case 4, the annular film occurs abruptly after 1.4 s and it indicates that a significant dry-out has occurred. Compared with the corresponding continuous annular flow, it worsens the heat transfer performance. On the other hand, the continuous flow pattern is stratified-wavy for case 3; however, the pulsations give rise to annular flow intermittently, thereby increasing heat transfer performance.

Table 1: Visualization of continuous and pulsatile flow upon a valve opening (BTS/ATS = before/after test section)

[s]	Case 1: BTS, $G = 100$, $\dot{V}_w = 0.30$	Case 2: BTS, $G = 150$, $\dot{V}_w = 0.76$	Case 3: ATS, $G = 100$, $\dot{V}_w = 0.30$	Case 4: ATS, $G = 150$, $\dot{V}_w = 0.76$
Cont.				
0.00				
0.05				
0.1				
0.15				
0.20				
0.30				
0.40				
0.50				
0.60				
0.70				
0.80				
0.90				
1.00				
1.10				
1.20				
1.30				
1.40				
1.50				

4. DISCUSSION

In Section 2.1, the error of the predicted heat transfer coefficients was found to be 3.8 %. However, the highest heat transfer enhancements were even lower on average (3.2 %) at low cycle times (1 s to 2 s). It is therefore difficult to validate if there is an enhancement using the flow pulsations. This question is dealt with in more detail in part 2 of this paper using statistical analysis. On the other hand, the performance was shown to be similar for both continuous and pulsatile flow. Only, at very high heat flux and cycle times, the liquid film dries-out significantly when the valve is closed.

It is common practice for horizontal flow boiling in traditional size tubing to measure wall temperatures at least with 4 locations circumferentially. However, given our future research activities on extending the test section to cover the full evaporation region, and test effects of flow pulsation further downstream the evaporator, we reduced the number of wall thermocouples so far. Next version of the test sections will include 4 wall temperatures circumferentially. It might show little effect on the actual heat transfer coefficient values, but their comparison (pulsation vs. continuous flow) is believed to be the same.

5. CONCLUSION

This paper presents an experimental comparison of flow boiling heat transfer in an 8 mm round tube with and without fluid flow pulsation for R134a, i.e. using a flow modulating expansion valve and a stepper motor continuous flow valve. The mass flux ranged from 41 kg/m²s to 167 kg/m²s, vapor quality from 0.18 to 0.59 and heat flux from 1.5 kW/m² to 45 kW/m². For these conditions, the results indicated that the nucleate boiling contribution dominated over the convective boiling contribution to flow boiling. Moreover, it was found that the flow pulsations improve the heat transfer coefficient by 3.2 % on average at low cycle times (1 s to 2 s). However, at higher cycle times (5 s to 9 s) the performance is much similar to that of continuous flow boiling. If the cycle time and the heat flux are high ($q \geq 35$ kW/m²), the flow pulsations may result in dry-out of the liquid film and consequently lower time-averaged heat transfer coefficient, i.e. as much as 8 %.

REFERENCES

- Antonenko, V.A., Chistyakov, Y.G., Kudritskiy, G.R., 1992. Vibration-aided boiling heat transfer. *Heat Transf. Res.* 24, 1147 – 1151.
- Bergles, A.E., 2003. High-flux processes through enhanced heat transfer, in: Rohsenow Symposium on Future Trends in Heat Transfer. Massachusetts, USA.
- Bohdal, T., Kuczyński, W., 2005. Investigation of Boiling of Refrigeration Medium Under Periodic Disturbance Conditions. *Exp. Heat Transf.* 18, 135–151. doi:10.1080/08916150590953379
- Chen, C.A., Chang, W.R., Lin, T.F., 2010. Time periodic flow boiling heat transfer of R-134a and associated bubble characteristics in a narrow annular duct due to flow rate oscillation. *Int. J. Heat Mass Transf.* 53, 3593–3606. doi:10.1016/j.ijheatmasstransfer.2010.02.038
- Kline, S.J., McClintock, F.A., 1953. Describing uncertainties in Single-Sample experiments. *Mech. Eng.* 75, 3–8.
- Kuczyński, W., Charun, H., Bohdal, T., 2012. Influence of hydrodynamic instability on the heat transfer coefficient during condensation of R134a and R404A refrigerants in pipe mini-channels. *Int. J. Heat Mass Transf.* 55, 1083–1094. doi:10.1016/j.ijheatmasstransfer.2011.10.002
- Obinelo, I.F., Round, G.F., Chang, J.S., 1994. Condensation enhancement by steam pulsation in a reflux condenser. *Int. J. Heat Fluid Flow* 15, 20–29. doi:10.1016/0142-727X(94)90027-2
- Ohadi, M.M., Dessiatoun, S. V., Darabi, J., Salehi, M., 1996. Active Augmentation of Single-Phase and Phase-Change Heat Transfer - an overview, in: Manglik, R.M., Kraus, A.D. (Eds.), *Process, Enhanced, and Multiphase Heat Transfer*. Begell House, New York, USA, pp. 277–286.

- Roh, C.W., Kim, M.S., 2012. Enhancement of heat pump performance by pulsation of refrigerant flow using a solenoid-driven control valve. *Int. J. Refrig.* 35, 1547–1557. doi:10.1016/j.ijrefrig.2012.04.018
- Ruspini, L.C., Marcel, C.P., Clausse, A., 2014. Two-phase flow instabilities: A review. *Int. J. Heat Mass Transf.* 71, 521–548. doi:10.1016/j.ijheatmasstransfer.2013.12.047
- Wedekind, G.L., 1971. An experimental investigation into the oscillatory motion of the mixture-vapor transition point in horizontal evaporating flow. *Trans. ASME. Ser. C, J. Heat Transf.* 93, 47 – 54.
- Wojtan, L., Ursenbacher, T., Thome, J.R., 2005. Investigation of flow boiling in horizontal tubes: Part II—Development of a new heat transfer model for stratified-wavy, dryout and mist flow regimes. *Int. J. Heat Mass Transf.* 48, 2970–2985. doi:10.1016/j.ijheatmasstransfer.2004.12.013

ACKNOWLEDGEMENT

This research was supported by the Danish Council for Independent Research | Technology and Innovation, (11-117025).